Generalised Atmospheric Rosenbluth Methods (GARM)

A. Rechnitzer[1,*] and E. J. Janse van Rensburg[2,†]

[1] *Department of Mathematics, University of British Columbia, Canada*
[2] *Department of Mathematics and Statistics, York University, Canada*

(Dated: June 18, 2008)

We show that the classical Rosenbluth method for sampling self-avoiding walks [1, 2] can be extended to a general algorithm for sampling many families of objects, including self-avoiding polygons. The implementation relies on an elementary move which is a generalisation of kinetic growth; rather than only appending edges to the endpoint, edges may be inserted at any vertex providing the resulting objects still lie within the same family. We implement this method using pruning and enrichment [3] to sample self-avoiding walks and polygons. The algorithm can be further extended by mixing it with length-preserving moves, such pivots and crank-shaft moves.

PACS numbers: 05.10.Ln,61.41.+e,87.15.ak

Monte Carlo simulations of self-avoiding walks (SAWs) and self-avoiding polygons (SAPs) on regular lattices are a major tool for the study of polymer statistics [4]. While kinetic growth algorithms [1, 2] have been used to sample SAWs to great success, it is unclear how they might be applied to SAPs. SAPs are models of ring polymers, plasmids (mitochondrial DNA) [5–7] and appear in the zero-component limit of the N-vector model [8]. In this paper, we generalise a growth algorithm for SAWs and show how it may be used to sample SAPs and other objects.

The Rosenbluth method for sampling self-avoiding walks (SAWs) is a classical algorithm dating back to the 1950s [1, 2]. This method found new application with the development of a pruned and enriched implementation, called PERM, due to Grassberger [3]. This was in turn further extended using flat-histogram and multicanonical methods [9, 10]. These new algorithms have found many applications in the modelling of polymers (eg.[11–13]).

The Rosenbluth method samples SAWs by growing conformations from a single vertex and iteratively adding edges from the final vertex to its unoccupied nearest neighbours. Let ω be a SAW of n edges and let m_k be the number of unoccupied nearest neighbour vertices of its endpoint when it is truncated after k edges (after the k^{th} iteration). The probability of sampling ω is given by

$$\Pr(\omega) = \prod_{k=1}^{n} m_{k-1}^{-1}. \tag{1}$$

If $m_k = 0$ the conformation is trapped and a new conformation is started. This attrition makes it difficult to sample long SAWs and sampling by this method is not uniform. The sample bias can be removed by weighting each SAW by $W(\omega) = \Pr(\omega)^{-1}$. The mean weight of all SAWs of length n is

$$\sum_{|\omega|=n} W(\omega)\Pr(\omega) = c_n \tag{2}$$

where c_n is the number of SAWs of length n. Thus one can estimate the number of conformations by computing the average weight of sampled SAWs. Sample averages of observables are computed by taking weighted averages.

The original Rosenbluth algorithm converges very slowly because of attrition and the large variance in weights of longer SAWs. Grassberger's pruned and enriched implementation [3] constituted a major advance that allows the algorithm to reduce these effects. This significantly improves its efficiency and applicability.

In this paper we demonstrate how the Rosenbluth algorithm can be generalised; SAWs can be sampled by inserting edges at any vertex rather than only at the endpoint. This idea may be extended to a growth algorithm for SAPs and other lattice objects. We also show how to combine it with length preserving moves such as pivots.

Atmospheres

Let ω be a SAW on the square lattice, starting from the origin. A *positive endpoint atmospheric edge* of ω is an edge on the lattice that can be appended to the last vertex of ω to extend its length by one while respecting self-avoidance (see Figure 1). The size of the positive atmosphere of ω, $a_+(\omega)$, is the number of positive atmospheric edges. We abuse our notation and use

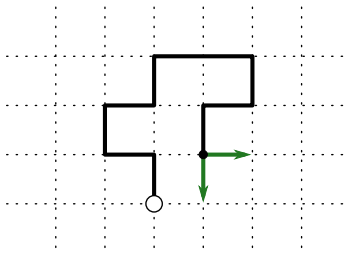

FIG. 1: A SAW and its two positive endpoint atmospheric edges.

*Electronic address: andrewr@math.ubc.ca
†Electronic address: rensburg@yorku.ca

a_+ to denote both the set of positive atmospheric edges and its size. Adding positive endpoint atmospheric edges increases the length of the SAW.

Appending a positive atmospheric edge to ω to obtain ω' creates a linkage (ω, ω') (see Figure 2). Deleting the last edge from ω' gives ω; we define the *negative endpoint atmosphere* of ω' to be this edge. We denote the size of the negative atmosphere of ω' by $a_-(\omega')$ and we again abuse notation by also using this symbol to denote the set of such edges. In the present context $a_-(\omega') \equiv 1$, but below we consider more general positive and negative atmospheres.

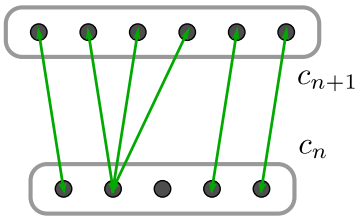

FIG. 2: A schematic picture of the linkages between c_n and c_{n+1}. There is one conformation with empty positive atmosphere.

By counting the number of linkages, we see that

$$\#\text{linkages} = \sum_{\omega} a_+(\omega) = \sum_{\omega'} a_-(\omega') = c_{n+1}. \tag{3}$$

This implies that

$$\frac{\langle a_+ \rangle_n}{\langle a_- \rangle_{n+1}} = \frac{c_{n+1}}{c_n} \tag{4}$$

where $a_-(\omega') \equiv 1$ and the averages are taken over the uniform distribution.

This observation can be used to estimate growth constants and free-energies of SAWs and bond trees [14–16]. We extend these definitions and show how they lead to a significant generalisation of the Rosenbluth algorithm.

Define the positive atmosphere, $a_+(\omega)$, to be the number of ways that an edge can be inserted into ω at any of its vertices so that a SAW is obtained (see Figure 3). Note that there are SAWs with empty positive atmosphere.

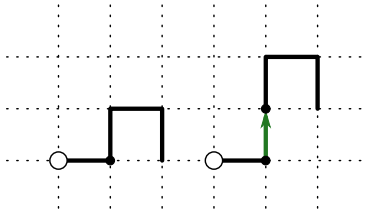

FIG. 3: The SAW on the right is obtained from the SAW on the left by inserting a north edge at the black vertex. This is one of its eleven positive atmospheric edges. It has three negative atmospheric edges.

Inserting a positive atmospheric edge into ω results in a new SAW, ω'. The negative atmosphere, $a_-(\omega')$, is the number of ways that an edge can be deleted to obtain a SAW. Linkages are created as above and equation (4) holds by the same arguments. Simulations show that the distribution of atmospheres are narrowly peaked (see Figure 4).

Generalised atmospheric Rosenbluth method

The generalised atmospheres, $a_\pm$, can be used to define a generalised Rosenbluth method for sampling SAWs. The algorithm starts with a single vertex, φ_0, and grows a sequence of SAWs, $\varphi = \varphi_0, \ldots, \varphi_n$, by inserting a positive atmospheric edge at each iteration. The conformation φ_{k+1} is obtained from φ_k by inserting an edge chosen uniformly from the available positive atmospheric edges, $a_+(\varphi_k)$. We call this the Generalised Atmospheric Rosenbluth Method (GARM). This method generalises the percolation based algorithms for trees in [17, 18].

A *sequence* of $n+1$ SAWs, $\varphi = \varphi_0, \ldots, \varphi_n$, is obtained after n iterations with probability

$$\Pr(\varphi \,|\, \varphi_0) = \prod_{k=1}^{n} a_+(\varphi_{k-1})^{-1}. \tag{5}$$

Since a given conformation can be obtained in several different ways, this is *not* the probability of obtaining the last SAW in the sequence. As such we give a weight to the sequence of SAWS, not only to compensate for the non-uniform sampling probability, but also to take into account this degeneracy. The weight of a sequence of SAWs, $\varphi = \varphi_0, \ldots, \varphi_n$ is

$$W(\varphi) = \prod_{k=1}^{n} \frac{a_+(\varphi_{k-1})}{a_-(\varphi_k)} \tag{6}$$

if $n \geq 1$ and $W(\varphi) = 1$ if $n = 0$.

The mean weight of sequences of length $n+1$ is

$$\langle W \rangle_n = \sum_{\varphi} W(\varphi) \Pr(\varphi \,|\, \varphi_0) = c_n. \tag{7}$$

To see this, consider all the sequences that end in a particular SAW τ of length n. It suffices to show that

$$1 = \sum_{\varphi \to \tau} W(\varphi) \Pr(\varphi \,|\, \varphi_0) = \sum_{\varphi \to \tau} \prod_{k=1}^{n} a_-(\varphi_k)^{-1} \tag{8}$$

where the sums are over all sequences that end in τ. Note that one must consider all the possible choices of atmospheric edges, so that there are $n!$ sequences that end in the SAW made up of n east edges.

We reinterpret the product of negative atmospheres as the probability of returning to the single vertex under the following process. Starting at φ_n, we delete negative atmospheric edges from φ_k to obtain φ_{k-1} iteratively. The probability of realising φ_0 along the sequence φ is

$$\Pr(\varphi_0|\varphi) = \prod_{k=1}^{n} \Pr(\varphi_{k-1} \,|\, \varphi_k) = \prod_{k=1}^{n} a_-(\varphi_k)^{-1}. \tag{9}$$

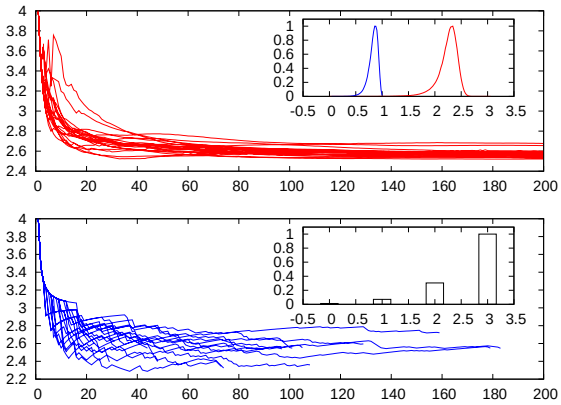

FIG. 4: Typical evolution of $W(\varphi)^{1/n}$ for both Rosenbluth and GARM sampling. Shown are 20 samples from each. While GARM does suffer from attrition, SAWs sampled by Rosenbluth have larger variance and a higher rate of attrition. The insets show the distributions of positive and negative atmospheres per vertex (top) and endpoint atmospheres (bottom); the peak heights have been normalised to 1.

Since all sequences that end at τ must return to φ_0 by this process, summing over φ gives equation (8) as required.

The above proof becomes trivial in the case of the endpoint atmosphere since $a_- \equiv 1$ and each SAW is obtained in exactly one way. The proof breaks down in models in which a given conformation cannot be reached by inserting positive atmospheric edges.

In Figure 5 we show that data obtained by a pruned and enriched implementation of GARM for SAWs agrees with exact enumeration data from [19]. We generated SAWs of a maximum of 200 edges with approximately 10^6 trajectories consisting of a total of 2.5×10^8 samples. This took about an hour on a laptop computer. This algorithm for the square-lattice generalises to SAWs on any graph with finite maximal degree.

Extensions to polygons, trees and animals

We now extend this algorithm to SAPs on the square lattice. In a previous paper, we defined the positive atmosphere to be the locations in which a single edge can be replaced by a $\sqcap$ conformation of three edges and the negative atmosphere was defined by the inverse of this process [20]. This definition is insufficient for GARM since there are many conformations that are not obtainable from the unit square; for example the 2×2 square.

We generalise the notion of positive atmospheres of SAPs by considering all the pairs of vertices at which anti-parallel edges may be inserted to obtain a longer SAP. The negative atmosphere is defined by finding all pairs of edges that may be removed to obtain a SAP. See Figure 6. All SAPs have non-zero positive atmosphere. Since the atmospheres now consist of pairs of edges we have

$$\frac{\langle a_+ \rangle_{2n}}{\langle a_- \rangle_{2n+2}} = \frac{p_{2n+2}}{p_{2n}} \tag{10}$$

where p_{2n} is the number of SAPs of length $2n$.

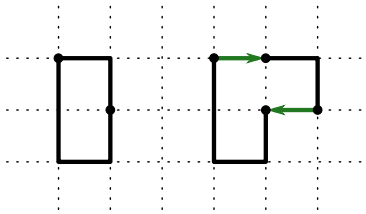

FIG. 6: A SAP and the insertion of a pair of anti-parallel edges. This SAP has positive atmosphere of 21 and negative atmosphere of 4.

In Figure 7 we show that data obtained by a PERM-like implementation of GARM for SAPs agrees with exact enumeration data from [21]. We generated SAPs of a maximum of 200 edges with approximately 4×10^5 trajectories consisting of a total of 5×10^7 samples. This took a few hours on a laptop computer.

This algorithm does not simply generalise to three dimensions with this definition of atmospheres. If φ_0 is chosen to be a unit square, then knotted conformations cannot be reached since inserting atmospheric edges does not allow strand passages.

GARM can be applied to lattice bond trees. The algorithm is then closely related to the algorithm in [17, 18]. In this case we define the positive atmosphere by looking

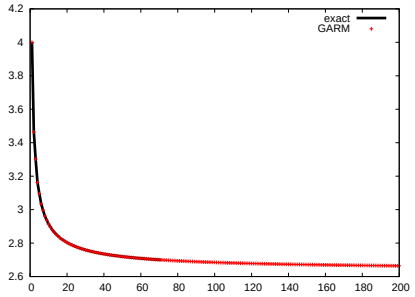

FIG. 5: A plot of $c_n^{1/n}$ as estimated from GARM data up to length 200. Exact enumeration data up to length 71 taken from [19] is shown for comparison.

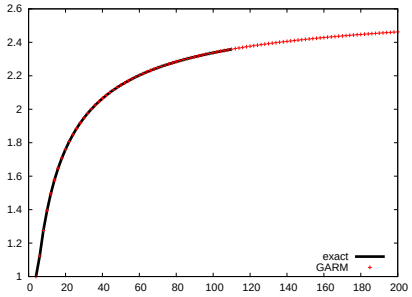

FIG. 7: A plot of $p_n^{1/n}$ as estimated from GARM data up to length 200 for even n. Exact enumeration data up to length 110 taken from [21] is shown for comparison.

at all the vertices at which an edge can be inserted to obtain a valid tree. When inserting an edge at a given vertex, one must be careful to consider all the possible ways of distributing the incident branches between both ends of the new edge. One may similarly define positive and negative atmospheres for animals. The positive atmosphere is defined by all the ways in which an edge may be inserted at vertices; unlike the tree case, some inserted edges will create cycles and so are double counted as they can be inserted from either vertex. The negative atmosphere is defined by the inverse of this process and atmospheric edges that are not cut-edges will be double counted. This algorithm works for site-trees; this may be easily implemented by defining positive and negative atmospheres in terms of leaves, but more general atmospheres are possible.

The implementation of the GARM algorithm requires rapid calculation of the positive and negative atmospheres. For SAWs the positive and negative atmospheres are $O(n)$ while for SAPs they are $O(n^2)$. At present we are able to compute the atmospheres in $O(n)$ time for SAWs and $O(n^2)$ for SAPs. Since the atmospheres must be computed at each iteration, the time to produce a conformation of length n is $O(n^2)$ and $O(n^3)$ for SAWs and SAPs respectively.

Conclusions

The definitions of atmospheres above were limited to positive and negative since they either increase or decrease the number of edges. We can generalise this further by including the notion of neutral atmospheric moves, a_0, which change the conformation without changing its size — for example a pivot move. At each iteration the algorithm chooses uniformly to add an edge from the positive atmosphere or to apply a neutral atmospheric move. The probability of obtaining a sequence φ is

$$\Pr(\varphi \,|\, \varphi_0) = \prod_{k=1}^{|\varphi|-1} \left(a_+(\varphi_{k-1}) + a_0(\varphi_{k-1})\right)^{-1}. \qquad (11)$$

and the corresponding weight is

$$W(\varphi) = \prod_{k=1}^{|\varphi|-1} \frac{a_+(\varphi_{k-1}) + a_0(\varphi_{k-1})}{a_-(\varphi_k) + a_0(\varphi_k)}. \qquad (12)$$

where $|\varphi|$ is the number of conformations in the sequence φ. The average weight of all sequences ending in a conformation of size n is c_n; the proof is as above. This addition makes it possible to sample SAPs in three dimensions and higher since the pivot algorithm is ergodic [22].

The algorithm can also be adapted to include Boltzmann factors (as per [3, 23]) so as to compute free energies. Further extensions such as multicanonical or flat histogram methods, such as those developed in [9, 10] are possible. We are currently investigating techniques to compute atmospheres more efficiently as this will improve the convergence of the GARM algorithm.

Acknowledgments

This paper was written while visiting the Erwin Schrödinger Institute in Vienna and thank them for their support. We acknowledge support from NSERC Canada in the form of Discovery Grants. We thank Juan Alvarez, Enzo Orlandini, Aleks Owczarek, Thomas Prellberg and Stu Whittington for discussions and comments.

[1] J. M. Hammersley and K. W. Morton, J. Roy. Stat. Soc. B **16**, 23 (1954).
[2] M. N. Rosenbluth and A. W. Rosenbluth, J. Chem. Phys. **23**, 356 (1955).
[3] P. Grassberger, Phys. Rev. E **56**, 3682 (1997).
[4] P. G. de Gennes, *Scaling Concepts in Polymer Physics* (Cornell University Press, 1979).
[5] V. Rybenkov, N. Cozzarelli, and A. Vologodskii, Proc. Natl. Acad. Sci. USA **90**, 5307 (1993).
[6] M. Gee and S. Whittington, J. Phys. A: Math. Gen. **30**, L1 (1997).
[7] B. Marcone, E. Orlandini, A. Stella, and F. Zonta, Phys. Rev. E **75**, 41105 (2007).
[8] K. Symanzik, Local Quantum Theory. AP, New York, London (1969).
[9] M. Bachmann and W. Janke, Phys. Rev. Lett. **91**, 208105 (2003).
[10] T. Prellberg and J. Krawczyk, Phys. Rev. Lett. **92**, 120602 (2004).
[11] M. S. Causo, B. Coluzzi, and P. Grassberger, Phys. Rev. E **62**, 3958 (2000).
[12] J. Krawczyk, A. L. Owczarek, and T. Prellberg, J. Stat. Mech.: Theo. Exp. p. P09016 (2007).
[13] H. P. Hsu, W. Paul, and K. Binder, Macromol. Symp. **252**, 58 (2007).
[14] A. Rechnitzer and E. J. Janse van Rensburg, J. Phys. A: Math. Gen. **35**, L605 (2002).
[15] E. J. Janse van Rensburg and A. Rechnitzer, Phys. Rev. E **67**, 36116 (2003).
[16] E. J. Janse van Rensburg and A. Rechnitzer, J. Phys. A: Math. Gen. **37**, 6875 (2004).
[17] C. M. Care and R. Ettelaie, Phys. Rev. E **62**, 1397 (2000).
[18] H. P. Hsu, W. Nadler, and P. Grassberger, J. Phys. A: Math. Gen. **38**, 775 (2005).
[19] I. Jensen, J. Phys. A: Math. Gen. **37**, 5503 (2004).
[20] E. J. Janse van Rensburg and A. Rechnitzer, J. Phys. A: Math. Theo. **41**, 105002 (2008).
[21] I. Jensen, J. Phys. A: Math. Gen. **36**, 5731 (2003).
[22] N. Madras, A. Orlitsky, and L. A. Shepp, J. Stat. Phys. **58**, 159 (1990).
[23] F. Seno and A. L. Stella, J. Phys. France **49**, 739 (1988).